SCIENTIFIC REPORTS

OPEN

SUBJECT AREAS:
FLUORESCENT PROBES
IMAGING STUDIES

Received
21 November 2014

Accepted
14 January 2015

Published
16 February 2015

Correspondence and requests for materials should be addressed to J.Y. (yinj@mail.ccnu.edu.cn) or J.Y. (jyoon@ewha.ac.kr)

Visualization of Endogenous and Exogenous Hydrogen Peroxide Using A Lysosome-Targetable Fluorescent Probe

Dabin Kim[1], Gyoungmi Kim[1], Sang-Jip Nam[1], Jun Yin[1,2] & Juyoung Yoon[1]

[1]Department of Chemistry and Nano Science, Ewha Womans University, Seoul 120-750, Korea, [2]Key Laboratory of Pesticide and Chemical Biology, Ministry of Education, College of Chemistry, Central China Normal University, Wuhan, 430079, P. R. China.

Reactive oxygen species (ROS) play crucial roles in diverse physiological processes; therefore, the efficient detection of ROS is very crucial. In this study, we report a boronate-based hydrogen peroxide (H_2O_2) probe having naphthalimide fluorophore. This probe also contained a morpholine moiety as a directing group for lysosome. The recognition property indicated that the probe exhibited high selectivity towards H_2O_2 not only in the solution but also in the living cells. Furthermore, it was used to monitor the level of endogenous and exogenous H_2O_2. These results support that the probe can function as an efficient indicator to detect H_2O_2.

Reactive oxygen species (ROS) are known to play key roles in the pathogenesis of serious diseases including cancer, neurodegenerative disorders, and cardiovascular diseases[1–3]. Therefore, efficient monitoring of the level of ROS in the living cells and tissues is very crucial for normal body functions and is helpful to estimate the biological processes[2–5] During the metabolism, the body produces a number of species derived from oxygen mainly including superoxide ($\cdot O_2^-$), hydroxyl radical ($\cdot$OH), peroxyl radical ($\cdot$OOR), single oxygen ($^1O_2$), hypochlorous acid/hypochlorite (HOCl/ClO^-), and hydrogen peroxide (H_2O_2). Among them, H_2O_2 plays diverse physiological roles including host defense, immune responses, and cellular signal transduction[6]. Specifically, increased concentrations of H_2O_2 may cause oxidative damage of cellular proteins, ageing, and diseases[7]. Therefore, the detection of H_2O_2 in living cells has been developed as a popular area in biological and chemical researches[8–11]. Undoubtedly, the chemical probes based on the fluorescence signal transduction provide a visualization tool for H_2O_2 detection.

Boronate has been known to efficiently react with H_2O_2 under weak alkaline condition to generate phenol[12]. Furthermore, the negative charge on the phenolate is easy to transfer to carbamate, forming unprotected amine[13]. Therefore, *p*-dihydroxyborylbenzyloxycarbonyl moiety has become one of the most efficient reactive groups with H_2O_2. In recent decade, fluorescent probes have been widely employed with different fluorophores, which were successfully applied in various living cells and tissues for monitoring the H_2O_2-induced biological process[14–21]. However, detecting H_2O_2 in some special organelles such as in lysosome is still very challenging. In addition, ROS can yield reactive products that accumulate and contribute to aging and disease in the process of catalyzing metals of body with proteins. For instance, the accumulation of peroxidized lipids and proteins in lysosomes of the brain cells can result in Alzheimer disease[22]. Simultaneously, the dismutation of peroxy radical ($\cdot O_2^-$) can generate H_2O_2, which is also a precursor of hypochlorous acid[23]. Therefore, the efficient monitoring and detection of H_2O_2 in lysosomes is significant in physiology and clinical diagnosis.

Toward this purpose, herein, we present a lysosome-targetable fluorescent probe based on naphthalimide fluorophore by using a popular *p*-dihydroxyborylbenzyloxycarbonyl moiety as a transponder. We investigated its optical properties and response toward various ROS and reactive nitrogen species. The result suggests that it possesses impressively high selectivity towards H_2O_2. The cell imaging confirmed that it can be used effectively as an indicator to monitor the level of H_2O_2 in lysosomes.

Results and Discussion

Design and synthesis. In usual, accurate method for the detection of species in special location of the cells is very crucial. In this case, we used morpholine an accepted directing group, which has been widely applied in the guidance of lysosomes[24–28]. In addition, *p*-dihydroxyborylbenzyloxycarbonyl has been proved to be an efficient

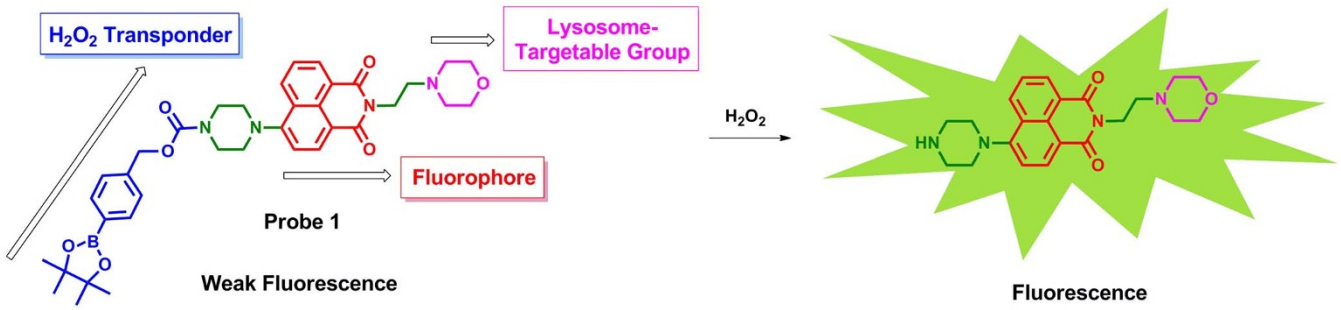

Figure 1 | **The structure of lysosome-targetable H_2O_2 probe 1.**

moiety for the detection of H_2O_2. Similarly, it was also selected as a transponder in this study case. Therefore, morpholine and *p*-dihydroxyborylbenzyloxycarbonyl moieties were introduced into the naphthalimide, as shown in Figure 1.

The synthetic route of probe **1** is outlined in Figure 2. As shown, commercial bromide **2** as a starting material was treated with 2-morpholinoethanamine **3** in ethanol to afford the morpholine-modified naphthalimide bromide **4** in a high yield. Subsequent ammonization with piperazine generates the intermediate **6**, which is treated with boronate **9** synthesized by the reaction of compounds **7** and triphosgene **8** to yield the probe **1**. The structures of new intermediates and target molecule were well characterized by the standard spectroscopic techniques such as NMR spectroscopy and mass spectrometry (see the Supporting Information).

Optical properties. The photophysical properties of probe **1** (2 μM) were determined in phosphate-buffered saline (0.1 M PBS, pH 7.4, containing 1% DMF). The UV/vis absorption spectrum of probe **1** at 400 nm was recorded. A weak fluorescence signal with an emission maximum at 528 nm was induced at an excitation wavelength of 405 nm. Due to the introduction of boronate, subsequent investigation focused on the response of probe **1** toward various ROSs (200 μM). In the UV/vis absorption spectra, no significant changes were observed after incubation for 2 h with various ROSs such as H_2O_2, ·OH, $ONOO^-$, ·OOR, ·NO, ClO^-, and t-ROOH at 25°C (Figure S1 in the Supporting Information (SI)). However, an obvious increase in the fluorescence intensity was observed only when H_2O_2 was added under the same condition in comparison to other ROS, as shown in Figure 3(A), clearly indicating that probe **1** was highly selective for H_2O_2.

Subsequently, the fluorescent titration of probe **1** (2 μM) upon addition of H_2O_2 (0–100 eq.) in PBS (pH 7.4) solution containing 1% DMF was investigated. As shown in Figure 3(B), the H_2O_2 induced an obvious fluorescence enhancement along with the increasing H_2O_2. These results strongly suggested that probe **1** was highly selective for the detection of H_2O_2 in aqueous solution. Next, we investigated the time-dependent UV/vis absorption and fluorescence spectra of probe **1** (2 μM) with H_2O_2 (200 μM) in PBS buffer solution (0.1 M PBS, pH 7.4, containing, 1% DMF). Similarly, no obvious changes were observed in the UV/vis absorption spectra (Figure S2 in the SI). However, a gradual fluorescence enhancement was observed (Figure S3 in the SI). As a comparison, other ROS could not induce a significant fluorescence change even after incubating with H_2O_2 over 2 h.

Bioimaging in living cells. As described above, probe **1** with high selectivity toward H_2O_2 and good water solubility permitted its further application in the living cells. In view of the fact that boronate-based fluorescence probes could function as an indicator for other ROSs such as ClO^-, $ONOO^-$, and peroxide except for H_2O_2[29–33], first, we investigated the selectivity of probe **1** in the living cells toward H_2O_2. HeLa cells were incubated with probe **1** (5 μM), and then incubated with ClO^-, $ONOO^-$, and H_2O_2 (100 μM), respectively. As shown in Figure S4, only H_2O_2 could induce an obvious red emission, which further confirmed that probe **1** had high selectivity not only in the solution but also in the living cells.

The good biocompatibility of authorized probe **1** was employed to assess the level of exogenous and endogenous H_2O_2 in the living cells. The HeLa cells were costained with probe **1** and LysoTracker Blue DND-22, which is a commercially available marker for lysosomes in Figure 4. In Figure 4A, the confocal microscopic image of probe **1** shows a red emission (Left). Along with the addition of 100 (Middle) and 200 μM (Right), an obvious fluorescence enhancement was observed. The result confirmed that probe **1** could monitor the level of H_2O_2 in the living cells. The imaging in Figures 4B and 4D strongly indicated that the probe possesses good cell-permeability and can be efficiently localized to lysosomes, as observed in other probes with a similar lysosome-targeting moiety[24–28]. Similar cell experiments were performed in living NIH-3T3 cells. The confocal microscopic image

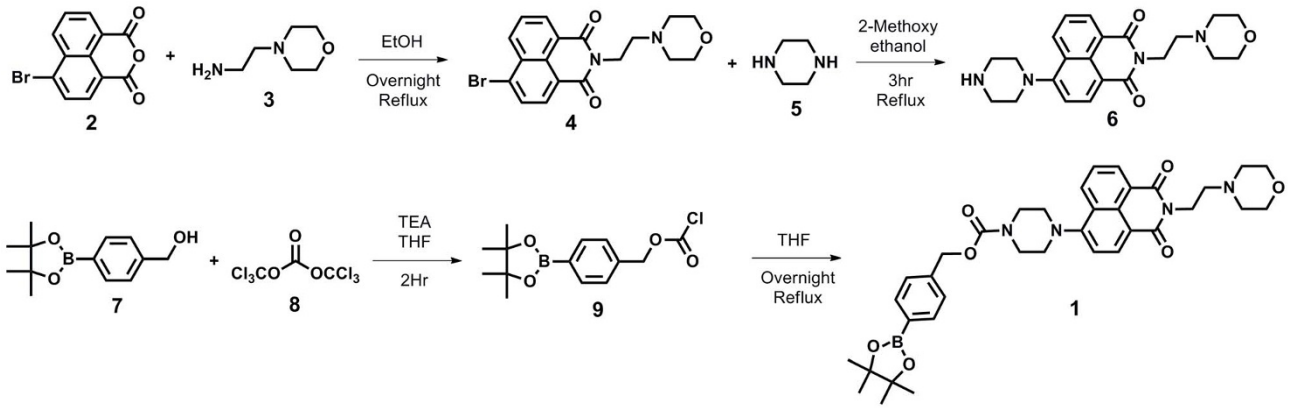

Figure 2 | **The synthesis of lysosome-targetable H_2O_2 probe 1.**

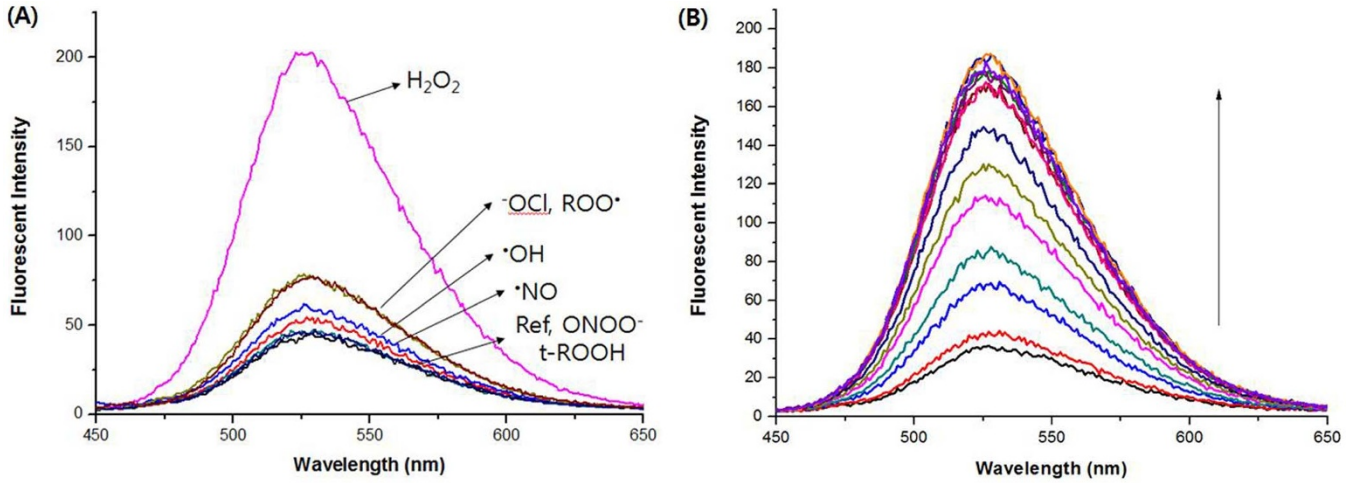

Figure 3 | (A) Fluorescence spectra of probe 1 (2 μM) with various ROS (200 μM) and (B) Fluorescent titration of probe 1 (2 μM) upon addition of H_2O_2 (0–100 eq.) in PBS (pH 7.4) solution containing 1% DMF after incubation for 2 h at 25°C at an excitation wavelength of 405 nm, and excitation and emission slit widths of 3 and 5 mm, respectively.

(Figure S5 in the SI) further confirmed that probe **1** is a lysosome-targetable H_2O_2 indicator. In view of H_2O_2 release from the cells and H_2O_2-induced biological processes, we used probe **1** to monitor the endogenous H_2O_2 in lysosome of the RAW 264.7 cells (Figure 5). As shown in Figure 5A (left), the confocal microscopic image of probe **1** shows a red emission owing to the existence of endogenous H_2O_2 released from the RAW 264.7 cells. For producing more endogenous H_2O_2, the RAW 264.7 cells were treated with PMA (Phorbol 12-myristate 13-acetate, 1 μg/mL). As might be expected, a significant fluorescence enhancement was observed (Figure 5A middle). Subsequent controllable experiments indicated that when TEMPO (2,2,6,6-tetramethylpiperidine-1-oxyl, 100 μM) was used as a ROS scavenger to block H_2O_2, decreasing in the fluorescence intensity (Figure 5A, right). These results in Figures 4 and 5 clearly indicate that lysosome-targetable probe **1** can be used as an efficient tool to monitor the level of exogenous and endogenous H_2O_2 in the living cells.

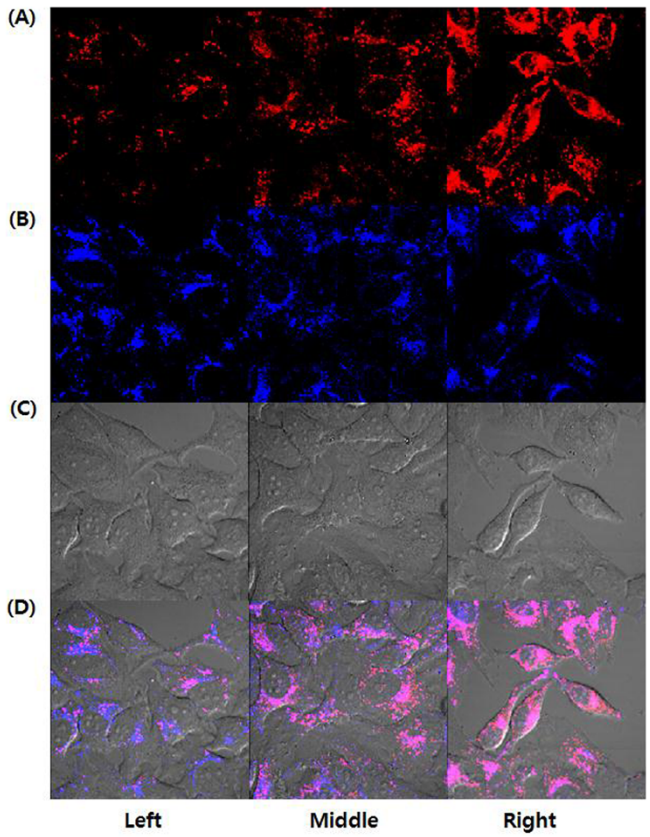

Figure 4 | **Probe 1 was localized to lysosomes in the HeLa cell.** Confocal microscopic images of probe **1** on the exogenous H_2O_2: (A) Probe **1** (red, ex405/em490–590 nm); (B) LysoTracker Blue DND-22 (blue, ex405/em430–455 nm); (C) Bright field (gray); (D) Overlay of (A) and (B) (purple). Left: No treatment; Middle: probe **1** + 100 μM H_2O_2; Right: probe **1** + 200 μM H_2O_2. (All the cells were stained with 5 μM probe **1**, 100 nM Lysotracker for 30 min and washed with DPBS and incubated with H_2O_2. Scale bar: 10 μm.).

Owing to its high selectivity and sensitivity, probe **1** was further subjected to explore the time-dependent fluorescence in the living cells. HeLa cells were incubated with 0 or 100 μM H_2O_2 for 30 min and then stained with probe **1** (0.2 μM). As shown in Figure 6A, the fluorescence image showed a weak red emission when the HeLa cells were not treated with H_2O_2. However, an increasing red emission was observed from the confocal microscopic images shown in Figure 6B when the HeLa cells were incubated with H_2O_2 (100 μM) as a result of the enhancement of fluorescence intensity as shown in Figure 6C, indicating that H_2O_2 could be easily captured by probe **1**. The result further suggests that probe **1** is an efficient indicator for monitoring the level of H_2O_2 in the living cells.

Reaction Mechanism. Understanding the sensor mechanism is very crucial for clarifying the optical properties. According to the similar reported mechanism[2], we supposed that probe **1** was possibly involved in the reaction shown in Figure 1. To further demonstrate the recognition mechanism of probe **1** for H_2O_2, first, we checked the mass. Probe **1** showed a peak at 655.3 (m/z) before adding H_2O_2 (Figure S6 in the SI). A new peak at 395.2 (m/z) (Figure S7 in the SI) was assigned to the cleavable product **6** (Figure 1). Moreover, the HPLC of probe **1** and compound **6** showed two peaks at retention times of 8.62 and 6.00, respectively (Figure S8 in the SI). After addition of H_2O_2, the peak at 8.62 min disappeared along with the appearance of a new peak at 6.41 min, which further confirmed our hypothesis. Next, we investigated the time-dependent reaction between probe **1** and H_2O_2 by HPLC, which showed that the reaction finished in 90 min (Figure S9 in the SI). Despite the cleavable product **6** was found in the reaction of probe **1** and ClO^- and $ONOO^-$, respectively (Figure S10 and S11 in the SI), there was

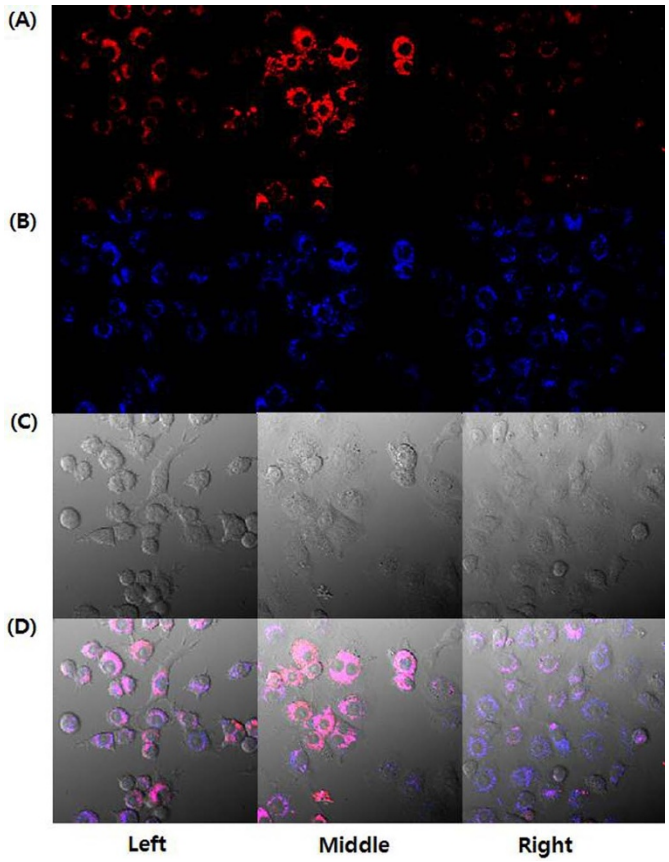

Figure 5 | Probe 1 was localized to lysosomes in RAW 264.7 cell. Confocal microscope images of probe **1** on the endogenous H_2O_2: (A) Probe **1** (red, ex405/em490–590 nm); (B) LysoTracker Blue DND-22 (blue, ex405/em430–455 nm); (C) Bright field (gray); (D) Overlay of (A) and (B) (purple). Left: No treatment; Middle: 1 μg/mL PMA (Phorbol 12-myristate 13-acetate), 1 h; Right: 1 μg/mL PMA, 1 h and 100 μM TEMPO (2,2,6,6-tetramethylpiperidine-1-oxyl, ROS scavenger), 1 h. (For producing endogenous H_2O_2, the RAW 264.7 cells were treated with PMA. All cells were stained with 5 μM probe **1,** 100 nM Lysotracker for 30 min. Scale bar: 10 μm.).

still much ROS in the system. These results further indicate that the probe **1** has high selectivity and sensitivity.

Consequently, a more detailed analysis of the structure and electron density was performed in an attempt to gain insight into its recognition mechanism. Accordingly, density functional theory (DFT) calculations were used to optimize the structures of probe **1** and compound **6** at the B3LYP/6-31G* level using a suite of Gaussian 09 programs. As shown in Figure 7, the piperazine ring in probe **1** and compound **6** showed a stable chair conformation, which was similar to our previous study[34]. For the probe **1**, the electron density mainly focused on the morpholine unit in its HOMO orbital. In its excited state (LUMO orbital), the electron transfer occurs to the naphthalimide unit. The classic proton-induced electron transfer (PET) indicated that probe **1** had a weak fluorescence. While the cleavable product **6** was only involved in the part of electron transfer from piperazine ring to naphthalimide in Figure 7B, the main electron density focused on the naphthalimide moiety and piperazine units. Therefore, the cleavable product **6** was fluorescent. Moreover, the calculated HOMO−LUMO energy gap of probe **1** was 3.02 eV, which was lower in comparison to **6**.

Conclusion

In conclusion, we prepared a boronate-based hydrogen peroxide probe using naphthalimide as the fluorophore and morpholine moiety as the directing group, displaying high selectivity toward H_2O_2 not only in the solution but also in the living cells. The results of the cell imaging suggested that it can be used to efficiently monitor the level of endogenous and exogenous H_2O_2. Moreover, the time-dependent fluorescence bioimaging further confirmed that the probe can function as an efficient indicator for the detection of H_2O_2. This study provides an idea to monitor the changes of biological species in special cell tissues and may be helpful to promote its application in clinical medicine in the future.

Experimental

General Methods. All reactions and assembly processes were carried out under an argon atmosphere by using standard Schlenk techniques, unless otherwise stated. All starting materials and reagents were obtained commercially. ^{1}H and ^{13}C NMR spectra used $CDCl_3$ solutions and a Bruker AM-300 spectrometer with tetramethylsilane (TMS) as the internal standard. Mass spectra were measured in the FAB mode. UV−vis spectra were obtained using a Scinco 3000 spectrophotometer (1 cm quartz cell) at 25°C. Fluorescence spectra were recorded on RF-5301/PC (Shimada) fluorescence spectrophotometer (1 cm quartz cell) at 25°C. Deionized water was used to prepare all aqueous solutions.

Synthesis of 4. 4-(2-aminoethyl)-morpholine **3** (1.00 g, 7.68 mmol) was added to a solution of 4-bromo-1,8-naphthalic anhydride **2** (1.00 g, 3.61 mmol) in anhydrous CH_3OH (20 mL) under nitrogen condition. The reaction mixture was refluxed for 8 hours and cooled down. After the residues was filtered, dried the yellowish filtered solid at room temperature in vacuum oven. Desired product was obtained as pale yellowish-white solid (yield 1.38 g, 98%). ^{1}H NMR ($CDCl_3$, 300 MHz): δ 8.65 (d,d, 1H), 8.57 (d,d, 1H), 8.40 (d, J = 8.1 Hz, 1H), 8.04 (d, J = 7.8 Hz, 1H), 7.85 (t, J = 7.2 Hz, 1H), 4.33(t, J = 6.9 Hz, 2H), 3.67 (t, J = 4.5 Hz, 4H), 2.70 (t, J = 7.2 Hz, 2H), 2.58 (t, J = 4.5 Hz, 4H). ^{13}C NMR ($CDCl_3$, 75 MHz) δ163.64, 163.62, 133.33, 132.05, 131.24, 131.13, 130.68, 130.34, 129.07, 128.10, 123.08, 122.21, 67.02, 67.02, 56.08, 53.81, 37.31. ESI-MS m/z = 389.0 $[M + H]^+$, calcd for 389.0.

Synthesis of 6. Compounds **4** (0.60 g, 1.54 mmol) and piperazine anhydrous **5** (0.27 g, 3.08 mmol) were dissolved in methoxyl ethanol (10 mL) under nitrogen

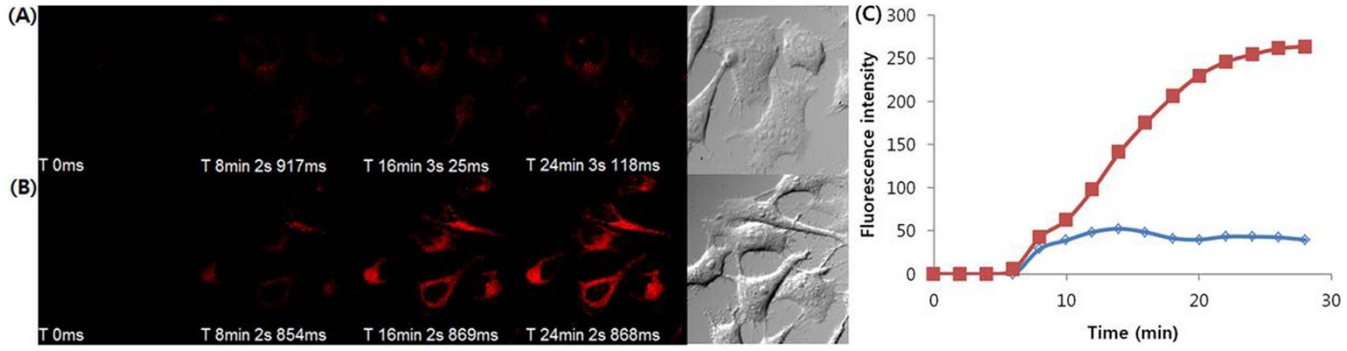

Figure 6 | Time-dependent fluorescence intensity of probe 1 in HeLa cells. HeLa cells were incubated with 0 or 100 μM H_2O_2 for 30 min and added 0.2 μM probe **1** for 30 min. The time-dependent fluorescence image of probe **1** was acquired by confocal microscopy: (A) no treatment; (B) 100 μM H_2O_2; (C) Time-dependent fluorescence intensity graph of probe **1** in HeLa cells. (Blue color: no treatment; Red color: 100 μM H_2O_2).

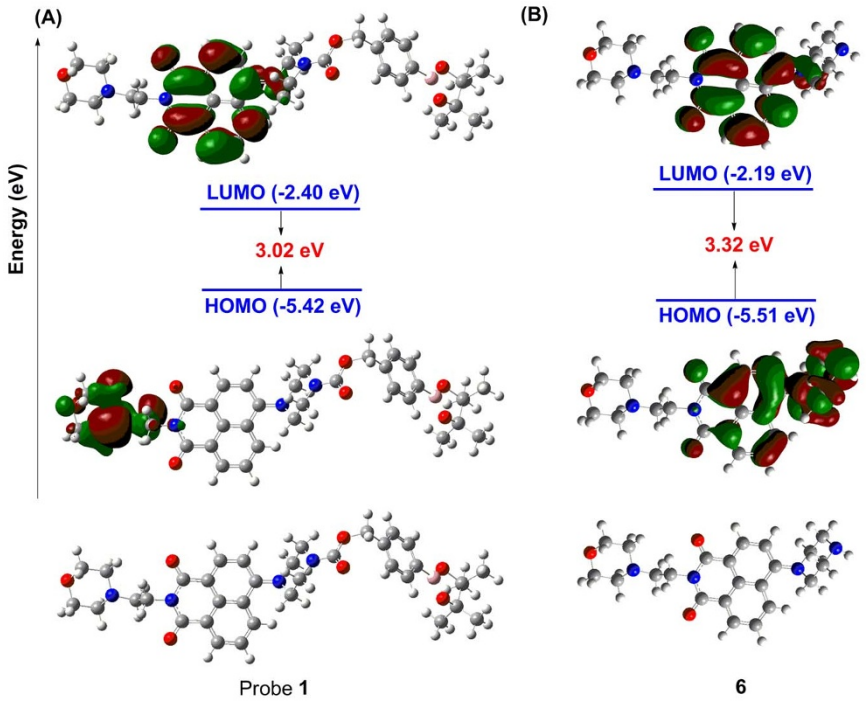

Figure 7 | Frontier molecular orbital profiles of 1 and 6 based on DFT (B3LYP/6-31G*) calculations.

condition. The reaction mixture was refluxed for 3 hours and cooled down. Then the solvent was removed under reduced pressure. The residue was purified by silica gel column chromatography using CH_2Cl_2/MeOH (10 : 1, v : v) as the eluent. Desired product was obtained as yellow solid (yield 0.40 g, 66%). ^{1}H NMR ($CDCl_3$, 300 MHz): δ 8.57 (d of d, J = 7.2 Hz, 1H), 8.51 (d, J = 8.1 Hz, 1H), 8.42 (d of d, J = 8.4 Hz, 1H), 7.69 (d of d, J = 8.4 Hz, 1H), 7.21 (d, J = 8.1 Hz, 1H), 4.32(t, J = 6.9 Hz, 2H), 3.68 (t, J = 4.5 Hz, 4H), 3.23 (d, J = 5.7 Hz, 4H), 3.22 (d, J = 5.7 Hz, 4H), 2.69 (t, J = 6.9 Hz, 2H), 2.59 (t, J = 4.5 Hz, 4H). ^{13}C NMR ($CDCl_3$, 125 MHz) δ 164.75, 164.26, 156.69, 132.85, 131.43, 130.62, 130.20, 126.46, 125.87, 123.45, 116.75. 115.20, 67.28, 56.44, 54.65, 54.04, 47.07, 46.94, 46.46, 45.70, 41.48, 37.32. FAB-MS m/z = 395.21 $[M + H]^+$, calcd for 395.21.

Synthesis of probe 1. Compounds **6** (0.19 g, 0.48 mmol) and **9**[35] (0.10 g, 0.32 mmol) were dissolved in anhydride THF (10 mL) and refluxed overnight. After removing the solvent, the residue was purified by silica gel column chromatography using CH_2Cl_2/MeOH (10 : 1, v : v) as the eluent to afford pure product **1**. Desired product was obtained as yellow solid (yield 0.10 g, 47%). ^{1}H NMR ($CDCl_3$, 300 MHz): δ 8.59 (d of d, J = 7.2 Hz, 1H), 8.52 (d, J = 8.1 Hz, 1H), 8.41 (d of d, J = 8.4 Hz, 1H), 7.82 (d, J = 8.1 Hz, 2H), 7.72 (d of d, J = 8.4 Hz, 1H), 7.39 (d, J = 8.1 Hz, 2H), 7.22 (d, J = 8.1 Hz, 1H), 5.20 (s, 2H), 4.33 (t, J = 6.9 Hz, 2H), 3.83 (s, 4H), 4.68 (t, J = 4.5 Hz, 4H), 3.22 (s, 4H), 2.69 (t, J = 6.9 Hz, 2H), 2.59 (s, 4H), 1.34 (s, 12H). ^{13}C NMR ($CDCl_3$, 75 MHz): δ 164.41, 155.49, 155.20, 139.44, 135.04, 132.46, 131.26, 129.87, 128.87, 127.21, 126.31, 126.07, 123.30, 117.39, 115.39, 83.90, 77.22, 67.39, 67.05, 56.19, 53.81, 52.88, 30.95, 24.86. FAB-MS m/z = 655.33 $[M + H]^+$, calcd for 655.33.

Cell culture. HeLa cells (human epithelial adenocarcinoma), NIH-3T3 (mouse fibroblast) and RAW 264.7 cells (mouse macrophage cell) were obtained from Korean Cell Line Bank (Seoul, Korea). Cells were cultured in RPMI 1640 (Roswell Park Memorial Institute, without HEPES) supplemented with heat-inactivated 10% fetal bovine serum, 100 U/ml penicillin and 100 U/ml streptomycin. NIH- 3T3 cells were cultured in DMEM (Dulbecco's Modified Eagle's Medium) supplemented with heat-inactivated 10% bovine calf serum, 100 U/ml penicillin and 100 U/ml streptomycin. All cells were kept in 5% CO_2 at 37°C.

Confocal microscopy imaging[36–38]**.** Cells were seeded in a 35-mm glass bottomed dishes at a density of 3 × 10^5 cells per dish in culture media. After 24 h, 5 μM probe **1** sensor and 100 nM Lysotracker Blue DND-22 added to the cells and the cells were incubated for 30 min at 37°C. For HeLa cells and NIH-3T3 cells, 100, 200 μM H_2O_2 added to the cell medium for 30 min and acquired images by confocal microscopy. For RAW 264.7 cells, 1 μg/ml PMA (phorbol 12-myristate 13-acetate) treated for 1 h and coincubated with 5 μM probe **1** for 30 min. For the inhibition test, 100 μM TEMPO (2,2,6,6-tetramethylpiperidine-1-oxyl) treated to the media for 1 h with PMA. After washing with the DPBS twice to remove the residual probe, the cells were imaged by confocal laser scanning microscopy (FV1200, Olympus, Japan). Cells were excited by a 405 nm diode laser and detected at BA 430–455 nm (Lysotracker), 490–590 nm (probe **1**). For ROS selectivity in the cells, cells were incubated with 5 μM probe **1** for 30 min and washed with DPBS and incubated with 100 μM H_2O_2, OCl^-, $ONOO^-$ for 30 min and acquired images by confocal microscopy.

1. Dixon, S. J. *et al.* The role of iron and reactive oxygen species in cell death. *Nat. Chem. Bio.* **10**, 9–17 (2014).
2. Chen, X. *et al.* Fluorescent and luminescent probes for detection of reactive oxygen and nitrogen species. *Chem. Soc. Rev.* **40**, 4783–4804 (2011).
3. Zhou, X., Kwon, Y., Kim, G., Ryu, J. & Yoon, J. A ratiometric fluorescent probe based on a coumarin-hemicyanine scaffold for sensitive and selective detection of endogenous peroxynitrite. *Biosens. Bioelectron.* **64**, 285–291 (2015).
4. He, F., Feng, F., Wang, S., Li, Y. & Zhu, D. Fluorescence ratiometric assays of hydrogen peroxide and glucose in serum using conjugated polyelectrolytes. *J. Mater. Chem.* **17**, 3702–3707 (2007).
5. Chen, X. *et al.* A specific and sensitive method for detection of hypochlorous acid for the imaging of microbe-induced HOCl production. *Chem. Commun.* **47**, 4373–4375 (2011).
6. Abo, M. *et al.* Visualization of Phagosomal Hydrogen Peroxide Production by a Novel Fluorescent Probe That Is Localized via SNAP-tag Labeling. *Anal. Chem.* **86**, 5983–5990 (2014).
7. Bortolozzi, R. *et al.* Selective ratiometric detection of H_2O_2 in water and in living cells with boronobenzo[b]quinolizinium derivatives. *Chem. Commun.* **50**, 8242–8245 (2014).
8. Dickinson, B. C., Lin, V. S. & Chang, C. J. Chemical functionalization strategies for carbon dioxide capture in microporous organic polymers. *Nat. Prot.* **8**, 1249–1259 (2013).
9. Redy, O., Kisin-Finfer, E., Ferber, S., Satchi-Fainaro, R. & Shabat, D. Synthesis and Use of QCy7-derived Modular Probes for Detection and Imaging of Biologically Relevant Analytes. *Nat. Prot.* **9**, 27–36 (2014).
10. Sella, E. & Shabat, D. Hydroquinone-quinone oxidation by molecular oxygen: a simple tool for signal amplification through auto-generation of hydrogen peroxide. *Org. Biomol. Chem.* **11**, 5074–8 (2013).
11. Karton-Lifshin, N. *et al.* A Unique Paradigm for a Turn-ON Near-Infrared Cyanine-Based Probe: Non-Invasive Intravital Optical Imaging of Hydrogen Peroxide. *J. Am. Chem. Soc.* **133**, 10960–10965 (2013).
12. Miller, E. W. & Chang, C. J. Fluorescent probes for nitric oxide and hydrogen peroxide in cell signaling. *Cur. Opin. Chem. Bio.* **11**, 620–625 (2007).
13. Lo, L. C. & Chu, C. Y. Development of highly selective and sensitive probes for hydrogen peroxide. *Chem. Commun.* **21**, 2728–2729 (2003).
14. Albers, A. E., Okreglak, V. S. & Chang, C. J. A FRET-Based Approach to Ratiometric Fluorescence Detection of Hydrogen Peroxide. *J. Am. Chem. Soc.* **128**, 9640–9641 (2006).
15. Dickinson, B. C. & Chang, C. J. A Targetable Fluorescent Probe for Imaging Hydrogen Peroxide in the Mitochondria of Living Cells. *J. Am. Chem. Soc.* **130**, 9638–9639 (2008).
16. Srikun, D. *et al.* An ICT-Based Approach to Ratiometric Fluorescence Imaging of Hydrogen Peroxide Produced in Living Cells. *J. Am. Chem. Soc.* **130**, 4596–4597 (2008).

17. Dickinson, B. C., Huynh, C. & Chang, C. J. A Palette of Fluorescent Probes with Varying Emission Colors for Imaging Hydrogen Peroxide Signaling in Living Cells. *J. Am. Chem. Soc.* **132**, 5906–5915 (2010).
18. Li, C. *et al.* A General Strategy To Construct Fluorogenic Probes from Charge-Generation Polymers (CGPs) and AIE-Active Fluorogens through Triggered Complexation. *Angew. Chem. Int. Ed.* **51**, 455–459 (2012).
19. Lee, S. W. *et al.* Ratiometric Fluorescent Probes for Hydrogen Peroxide from a Focused Library. *Chem. Eur. J.* **19**, 14791–14794 (2013).
20. Xu, M. *et al.* A selective fluorescence turn-on sensor for trace vapor detection of hydrogen peroxide. *Chem. Commun.* **49**, 11779–11781 (2013).
21. Franks, A. T. & Franz, K. J. A prochelator with a modular masking group featuring hydrogen peroxide activation with concurrent fluorescent reporting. *Chem. Commun.* **50**, 11317–11320 (2014).
22. Devasagayam, T. P. *et al.* Free radicals and antioxidants in human health: current status and future prospects. *J. Assoc. Physicians. India.* **52**, 796–804 (804).
23. Sies, H. *Oxidative stress: introductory remarks* [Sies, H. (ed.)] [1–7] (Academic Press, London, 1985).
24. Yu, H., Xiao, Y. & Jin, L. A Lysosome-Targetable and Two-Photon Fluorescent Probe for Monitoring Endogenous and Exogenous Nitric Oxide in Living Cells. *J. Am. Chem. Soc.* **134**, 17486–17489 (2012).
25. Liu, T., Xu, Z., Spring, D. R. & Cui, J. A Lysosome-Targetable Fluorescent Probe for Imaging Hydrogen Sulfide in Living Cells. *Org. Lett.* **15**, 2310–2313 (2013).
26. Wang, L., Xiao, Y., Tian, W. & Deng, L. Activatable Rotor for Quantifying Lysosomal Viscosity in Living Cells. *J. Am. Chem. Soc.* **134**, 2903–2906 (2013).
27. Gao, M., Hu, Q., Feng, G., Tang, B. Z. & Liu, B. A fluorescent light-up probe with "AIE + ESIPT" characteristics for specific detection of lysosomal esterase. *J. Mater. Chem. B.* **2**, 3438–3442 (2014).
28. Yang, S. *et al.* Design of a Simultaneous Target and Location-Activatable Fluorescent Probe for Visualizing Hydrogen Sulfide in Lysosomes. *Anal. Chem.* **86**, 7508–7515 (2014).
29. Xu, Q. *et al.* A Highly Specific Fluorescent Probe for Hypochlorous Acid and Its Application in Imaging Microbe-Induced HOCl Production. *J. Am. Chem. Soc.* **135**, 9944–9949 (2013).
30. Sun, X. *et al.* A water-soluble boronate-based fluorescent probe for the selective detection of peroxynitrite and imaging in living cells. *Chem. Sci.* **5**, 3368–3373 (2014).
31. Kim, J., Park, J., Lee, H., Choi, Y. & Kim, Y. A boronate-based fluorescent probe for the selective detection of cellular peroxynitrite. *Chem. Commun.* **50**, 9353–9356 (2014).
32. Yu, F., Song, P., Li, P., Wang, B. & Han, K. A fluorescent probe directly detect peroxynitrite based on boronate oxidation and its applications for fluorescence imaging in living cells. *Analyst.* **137**, 3740–3749 (2012).
33. Wang, L. *et al.* A ratiometric fluorescent probe with excited-state intramolecular proton transfer for benzoyl peroxide. *RSC Adv.* **3**, 8674–8676 (2013).
34. Yin, J. *et al.* A Cyanine Based Fluorescence Probe for Highly Selective Detection of Glutathione in Cell Cultures and Live Mice Tis-sues. *J. Am. Chem. Soc.* **136**, 5351–535 (2014).
35. Lo, L. C. & Chu, C. Y. Development of highly selective and sensitive probes for hydrogen peroxide. *Chem. Commun.* **21**, 2728–2729 (2003).
36. Yuan, L., Lin, W., Xie, Y., Chen, B. & Zhu, S. Single Fluorescent Probe Responds to H_2O_2, NO, and H_2O_2/NO with Three Different Sets of Fluorescence Signals. *J. Am. Chem. Soc.* **134**, 1305–1315 (2012).
37. Humphries, J. E. & Yoshino, T. P. Regulation of hydrogen peroxide release in circulating hemocytes of the planorbid snail Biomphalaria glabrata. *Dev. Comp. Immunol.* **32**, 554–562 (2008).
38. Yuan, L. *et al.* A Unique Approach to Development of Near-Infrared Fluorescent Sensors for in Vivo Imaging. *J. Am. Chem. Soc.* **134**, 13510–13523 (2012).

Acknowledgments

This research was supported by a grant from the National Creative Research Initiative programs of the National Research Foundation of Korea (NRF) funded by the Korean government (MSIP) (No. 2012R1A3A2048814). Jun Yin also acknowledges financial support from National Natural Science Foundation of China (21402057).

Author contributions

J.Yin and J.Yoon designed the experiments. D.K. synthesized and characterized probe 1, and generated the data shown in Fig. 1–6. G.K. performed the cell experiments. J.Yin carried out the DFT calculation. S.-J.N., J.Yin and J.Yoon wrote the manuscript.

Additional information

Supplementary information accompanies this paper at http://www.nature.com/scientificreports

Competing financial interests: The authors declare no competing financial interests.

How to cite this article: Kim, D., Kim, G., Nam, S.-J., Yin, J. & Yoon, J. Visualization of Endogenous and Exogenous Hydrogen Peroxide Using A Lysosome-Targetable Fluorescent Probe. *Sci. Rep.* **5**, 8488; DOI:10.1038/srep08488 (2015).